Friction- and Mountain-Torque Estimates from Global Atmospheric Data

JOHN M. WAHR[1]

Geophysical Fluid Dynamics Program and Department of Geological and Geophysical Sciences, Princeton University, Princeton, NJ 08544

ABRAHAM H. OORT

Geophysical Fluid Dynamics Laboratory, NOAA, Princeton University, Princeton, NJ 08542

(Manuscript received 1 April 1983, in final form 26 September 1983)

ABSTRACT

Seasonal, zonal surface torques between the atmosphere and the earth are estimated and compared, using data from a number of independent sources. The mountain torque is computed both from surface pressure data and from isobaric height data. The friction torque is estimated from the oceanic stress data of Hellerman and Rosenstein. Results for the total torque are inferred from atmospheric angular momentum data. Finally, the globally integrated total torque is compared with astronomical observations of the earth's rotation rate. These comparisons help us to assess the quality of the different results.

Zonal torques are also computed using results from a GFDL general circulation model of the atmosphere. A comparison with the corresponding results inferred from real data is presented and interpreted in terms of model accuracy.

1. Introduction

The thermal and dynamical coupling between the atmosphere and the underlying solid earth and oceans plays an important role in determining the atmospheric circulation. The dynamical coupling is caused by surface tractions at the air–earth interface and can be separated into the effects of pressure (i.e., normal traction) and viscous or frictional shear (i.e., tangential traction).

A useful way to discuss this coupling and the accompanying circulation is in terms of the exchange of atmospheric angular momentum, as suggested by Starr (1948). In this formulation the surface coupling is perceived as an external torque on the atmosphere which causes a transfer of angular momentum between the atmosphere and the earth. The surface pressure forces are associated with the "mountain torque" (the surface torque due to unequal pressure on opposite sides of a topographic feature), and the surface frictional forces are responsible for the "friction torque". Since the atmospheric circulation is predominately zonal, most interest has focused on identifying the zonal component of the torque.

The zonal mountain torque in the midlatitude Northern Hemisphere was first estimated by White (1949) from sea-level and upper-air pressure data. In that study, as in most other studies of zonal torques (including this one), only the zonally averaged torque and only the seasonal cycle were considered. Newton (1971a) and Oort and Bowman (1974) used a slightly different method to estimate the zonal mountain torque which required isobaric height data from the global rawinsonde network.

A problem with both these methods of estimating mountain torques, is that the data resolution is not always compatible with the horizontal scale of the earth's topography. For example, the mountain torque caused by small-scale topographic features can not be reliably estimated (see Smith, 1978). Perhaps more serious is that some areas of large topographic gradients are also areas with limited data coverage. For example, the network of surface pressure data available from central Asia is sparse; and there are few rawinsonde stations in the mountainous regions of South America and Africa. There are, presumably, large mountain torques in these areas, but they may not be adequately determined by the present data.

Friction torque estimates require surface wind data plus an understanding of the relationship between surface winds and surface stress. That relationship is reasonably well understood over the ocean, but poorly known over land. On the other hand, surface wind data are fairly good over land but somewhat scattered over the ocean. As a result, existing friction torque estimates should be interpreted with caution.

Kung (1968) estimated zonal friction torques over

[1] Current affiliation: Department of Physics and Cooperative Institute for Research in Environmental Science, University of Colorado, Boulder, CO 80309.

the midlatitude Northern Hemisphere using geostrophically derived surface wind speeds and a regionally varying roughness parameter to model the seasonal friction stress over both land and ocean. Newton (1971b) constructed two estimates for the zonal friction torque over all latitude belts. In the first, oceanic friction stress data from Priestly (1951), Hidaka (1958) and Hellerman (1967) were used and extended over land by assuming that the average zonal friction torque over land at a given latitude was equal to the average zonal friction torque over the ocean at that same latitude. Although there is some physical motivation for this assumption (see Section 3), Newton found that this estimate, combined with his results for the mountain torque and the horizontal flux of atmospheric angular momentum, did not conserve angular momentum within the atmosphere. In Newton's second estimate, and the one he preferred, friction torque values were estimated over most of the globe as residuals from the other better known terms in the angular momentum balance.

One suggestion from all of these studies is that at most latitudes the friction torque may be as much as three to four times larger than the mountain torque, but that when averaged over either hemisphere, the friction torque and mountain torque have comparable magnitude (although not necessarily the same sign). There is also some indication that the mountain and friction torques have similar latitude dependence: latitudes with large eastward (westward) friction torques also have large eastward (westward) mountain torques.

The principle of angular momentum conservation implies that the total torque on the atmosphere is equal to the time rate of change of atmospheric angular momentum. Consequently, the total torque can be estimated indirectly using atmospheric angular momentum data. Angular momentum in the atmosphere can be separated into Ω-angular momentum and relative angular momentum:

$$M = M_\Omega + M_r = \Omega r^2 \cos^2\phi + ur\cos\phi,$$

where Ω = rotation rate of the earth, r = distance to the center of the earth, u = zonal wind component (positive if from west to east), and ϕ = latitude.

These two types of angular momentum correspond to an analogous separation of the inertial space velocity field into a rigid rotation of the atmosphere at one cycle per day, coincident with the mean rotation of the earth, plus a residual velocity field representing particle motion (i.e., winds) relative to the earth's surface. Changes in Ω-angular momentum are the result of a redistribution of mass within the atmosphere. Changes in the relative angular momentum are due mainly to variations in the atmospheric winds. Lorenz (1967) and Newton (1971b) concluded that seasonal changes in the zonal relative angular momentum were probably much larger than seasonal changes in the zonal Ω-angular momentum.

Widger (1949), Starr and White (1951), Newton (1971b), Newell *et al.* (1972), and Oort and Peixoto (1983) used rawinsonde observations to determine the flux and time rate of change of the zonal relative angular momentum, and then used the results to construct independent estimates for the total zonal torque on the atmosphere as a function of latitude. These indirect estimates of the total torque are, in a sense, more objective than the direct mountain torque and friction torque estimates discussed above. That is, the angular momentum estimates do not require assumptions about the nature of the interaction between the atmosphere and the earth. The angular momentum results are, however, subject to other errors, such as the limited rawinsonde data coverage, particularly over the Southern Hemisphere.

Since the estimates described above are all subject to potentially serious sources of error, it is not obvious to what extent the results are useful. We address this problem in the work presented below, by re-estimating the zonal torques using each of the different methods discussed above, and comparing results whenever appropriate. Estimates of the zonal mountain torque are obtained both from surface pressure data and from isobaric height data, and the results are compared in Section 2. The zonal friction torque is then estimated from surface stress data (Section 3), the results are added to the mountain torque estimates, and the resulting total torque is compared in Section 4 with the total torque estimates inferred from atmospheric angular momentum data. Finally, the total zonal torque, integrated over all latitudes, is compared in Section 4 with the astronomically observed seasonal variation in the earth's rotation. Since each estimate is subject to a different type of error, these comparisons can be used to assess the quality of the results. In a recent paper, Swinbank (1984) used a similar approach to study the atmospheric angular momentum balance during the Special Observing Periods of the First GARP Global Experiment.

One potentially useful application of this work is to compare the torque estimates computed from real data with corresponding estimates derived from a numerical model of the atmosphere. Since surface torques play an important role in the atmospheric circulation, this comparison can be of help in assessing the behavior of the numerically simulated atmosphere. We present such a comparison below, using results from two related atmospheric general circulation models constructed at the Geophysical Fluid Dynamics Laboratory (GFDL) in Princeton, New Jersey (see the discussion and references in Section 2). Model estimates are included in Sections 2, 3 and 4 for the mountain torque, friction torque and total torque, respectively. The agreement between the model results and the results inferred from real data is generally quite good. Some of the more important discrepancies which do exist can be explained in terms of known deficiencies in the model.

2. Mountain torque

The mountain torque on the atmosphere is the torque caused by differential pressure acting across topographic features on the earth's surface. Consider any arbitrary point on the surface of the earth with geocentric position vector $\mathbf{r}$, local outward normal $\hat{\mathbf{n}}$, and atmospheric pressure p_s (see Fig. 1 for a pictorial representation). The pressure force per unit area on the atmosphere at $\mathbf{r}$ is $p_s\hat{\mathbf{n}}$, and so the corresponding torque per unit area on the atmosphere is $\mathbf{r} \times (p_s\hat{\mathbf{n}})$. The normal, $\hat{\mathbf{n}}$, is given by

$$\hat{\mathbf{n}} = \hat{\mathbf{r}} - \nabla H(\phi, \lambda),$$

where $\hat{\mathbf{r}}$ is a unit vector in the radial direction, ϕ and λ are latitude and longitude, respectively, and $H(\phi, \lambda)$ is the departure of the earth's surface from spherical symmetry. The zonal component of the torque per unit area at $\mathbf{r}$ is then

$$\hat{\Omega} \cdot (\mathbf{r} \times p_s\hat{\mathbf{n}}) = r \cos\phi p_s n_\lambda = -p_s \frac{\partial H(\phi, \lambda)}{\partial \lambda}, \quad (1)$$

where $\hat{\Omega}$ is a unit vector along the earth's rotation axis and n_λ is the eastward component of $\hat{\mathbf{n}}$.

Departures from spherical symmetry, represented by the function H, are due not only to the earth's topography, but also to the earth's mean ellipticity of figure (which closely approximates the surface of mean sea level). In fact, most of the absolute departure from spherical symmetry comes from the earth's ellipticity: $H(\phi, \lambda)$ varies by over 20 km between the poles and the equator. This elliptical contribution to H is important in determining the meridional pressure torques. For example, the indications are that at the annual cycle the total globally integrated meridional torque due to pressure against the earth's elliptical bulge is roughly an order of magnitude larger than both the corresponding meridional mountain torque and the meridional friction torque (see, e.g., Wahr, 1983).

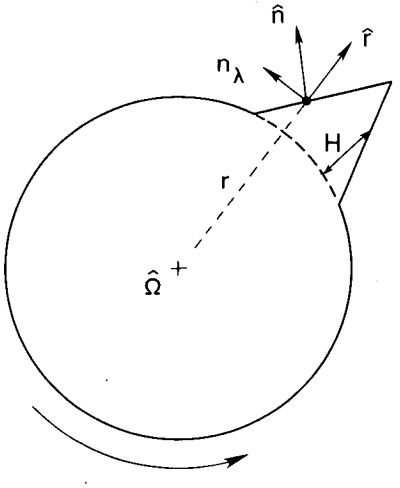

FIG. 1. A pictorial representation of the symbols used in Eq. (1). The figure is a representation of the earth with an exaggerated topographic feature, as seen from above the north pole. The unit vector $\hat{\Omega}$ is out of the page. The direction of the earth's rotation rate is indicated.

However, the elliptical contributions to H are independent of λ (an elliptical earth is zonally symmetric), and so equation (1) implies that the ellipticity has no effect on the zonal pressure torque. As a result, $H(\phi, \lambda)$ in (1) can be assumed, instead, to be the elevation of topography above local mean sea level.

The total zonal torque per degree latitude integrated around a belt of constant latitude is

$$T_M = \frac{-a^2\pi}{180} \cos\phi \int_0^{2\pi} p_s \frac{\partial H}{\partial \lambda}\, d\lambda, \quad (2)$$

where a is the mean radius of the earth and λ in the integrand is in radians. Integration by parts gives an alternate but equivalent result:

$$T_M = \frac{a^2\pi}{180} \cos\phi \int_0^{2\pi} H \frac{\partial p_s}{\partial \lambda}\, d\lambda. \quad (3)$$

We have used (2) to compute the annual mean and seasonal mountain torques from atmospheric pressure data. The raw pressure data consist of global, monthly station data from more than 2400 stations for January 1900 through April 1973, compiled by the National Climatic Center in Asheville, North Carolina. For a minority of stations, estimated sea-level pressure, rather than the actual surface pressure, is reported. The procedure for estimating sea-level pressure differs from one station to another, but as long as the station elevations are not too high, all procedures are well represented by (see, e.g., World Meteorological Organization, 1968)

$$\frac{p_0}{p_s} = \left(1 + \frac{\gamma H}{T_s}\right)^{g/R\gamma}, \quad (4)$$

where p_0 is the estimated sea level pressure, p_s, H, and T_s are the observed pressure, elevation, and temperature at the surface, g is the acceleration of gravity, R is the gas constant, and γ is the lapse rate. If a station reported only sea level pressure and if the station elevation was less than 1000 m, then we used (4), together with $\gamma = 0.005$ K m^{-1}, to estimate p_s from p_0 and T_s at that station. If a station reported only sea level pressure and its elevation was greater than 1000 m, the station was ignored.

Once the 1900–73 surface pressure data set was assembled, it was separated for each calendar month into two long-term mean subsets, one for January 1900 through April 1958, and the other for May 1958 through April 1973. The reason the data were organized into two sets was a matter of convenience, since the latter set was needed for another climatological study of the 1958–73 period (Oort, 1983). However, this separation into two seasonal data sets allowed us to

compare results from two independent samples and thereby to get some idea of the accuracy of the results.

The two seasonal data sets were smoothly interpolated to evenly spaced grid points (5° in longitude and 2.5° in latitude) over the globe. To minimize numerical errors in the interpolation procedure we first subtracted from every monthly-mean station report a time-independent constant, meant to approximate the expected time-averaged pressure at that station. This constant field, denoted here as the NMC standard pressure field (see, e.g., Oort, 1983, Table 7), is a function only of the station elevation. Since a pressure field which depends only on elevation should give no net contribution to T_M (to see this, let p_s in (2) be a function only of H), subtraction of this constant pressure field from the raw data should, in principle, have no effect on the mountain torque results. However, in practice, discrepancies may arise (see below).

The interpolation used here is an objective analysis scheme introduced by Thomasell and Welsh (1963) and discussed further in Rosen *et al.* (1979), Oort and Rasmussen (1971) and Oort (1983). In this method, grid point values for a given month are obtained by averaging data from neighboring stations. The field is then extended to grid points which have no nearby reporting stations by solving Poisson's equation at the unknown grid points and using the already averaged grid point values as fixed boundary values. The forcing term in Poisson's equation is the Laplacian of an appropriate initial guess field.

The two seasonal sets of analyzed pressure data were used in a discrete analogue of (2) to find two corresponding seasonal sets of latitude-dependent mountain torques, T_M. The height field, $H(\phi, \lambda)$, was taken from Smith *et al.* (1966) and was smoothed to have a horizontal resolution compatible with the resolution of the interpolated pressure field. The derivative of H with respect to longitude is approximated using a symmetrical difference:

$$\left(\frac{\partial H}{\partial \lambda}\right)_i d\lambda = \frac{1}{2}(H_{i+1} - H_{i-1}),$$

where the subscript i represents the longitudinal index of the grid. In this case, the discrete form of (2) at any latitude ϕ is

$$T_M = \frac{-a^2\pi}{180}\cos\phi \sum_i \frac{1}{2}(p_s)_i(H_{i+1} - H_{i-1}). \quad (5)$$

It is easy to show that if a corresponding symmetrical difference is used for the $\partial p_s/\partial\lambda$ derivative in (3), then the discrete versions of (2) and (3) are identical.

The mountain torque results were separated into an annual mean field and a seasonal departure from the annual mean. We found by comparing results from the 1900–58 and the 1958–73 data sets, that the annual mean results were not well determined by the surface pressure data. The discrepancy was particularly pronounced at latitudes between 25 and 45°N and between 0° and 25° S. The apparent explanation is a combination of two factors. First, the mountain torque in these two latitude belts is highly sensitive to the pressure distribution over central Asia (the Himalayas) and over the northern Pacific Coast of South America (the northern Andes), respectively. Unfortunately, station coverage in these areas was quite irregular (see Fig. 2 for the 1958–73 station distribution). Much of central Asia was poorly represented in both data sets, and, in fact, in this area many 1900–58 stations were not present in the 1958–73 data set, and vice versa. In the northern Andes station coverage was reasonably good during 1958–1973 but poor during 1900–58. (For a discussion of the quality of the pressure data in the Northern Hemisphere, see Trenberth and Paolino, 1980.)

Second, systematic errors can be introduced if the grid points are not symmetrically distributed with respect to the topography. Consider, for example, the local east–west topography shown in Fig. 3, with grid points A, B, C and D. Using this example in (5) and assuming, for simplicity, that $H = 0$ at grid points A and D, we find an apparent net eastward torque of

$$T_M = \frac{-a^2\pi}{360}\cos\phi[H_B(p_A - p_C) + H_C(p_B - p_D)], \quad (6)$$

where H_B and H_C are the elevations of points B and C; p_A, p_B, p_C, and p_D represent the surface pressures at A, B, C and D; and ϕ is the latitude of the cross section shown in Fig. 3. If the surface pressure depends only on the elevation, there should be no net mountain torque from this topography. In fact, it is easy to show that if p is a linearly decreasing function of H, the estimate (6) vanishes identically. However, if p were some nonlinear function of H and if $H_B \neq H_C$, then, in general, $T_M \neq 0$. This misrepresentation of the mountain torque is due, in this case, to the asymmetrical distribution of the points B and C with respect to the topography, and to the assumed nonlinear behavior of pressure with elevation.

For the real earth, it is convenient to divide the annual-mean surface pressure field into a dominant elevation dependent field and a much smaller residual field which is independent of elevation in some prescribed sense. The elevation-dependent field should produce no net mountain torque when averaged over any belt of constant latitude. However, if that field is not exactly linear with elevation, then computed results for T_M from that field are subject to these grid point errors. Subtraction of a standard pressure field as used at the National Meteorological Center (NMC) from the raw data before analysis should reduce this error (the NMC standard pressure field is not a strictly linear function of elevation). But departures from the NMC standard field are still apt to be present in the elevation dependent field, and these will cause errors. This prob-

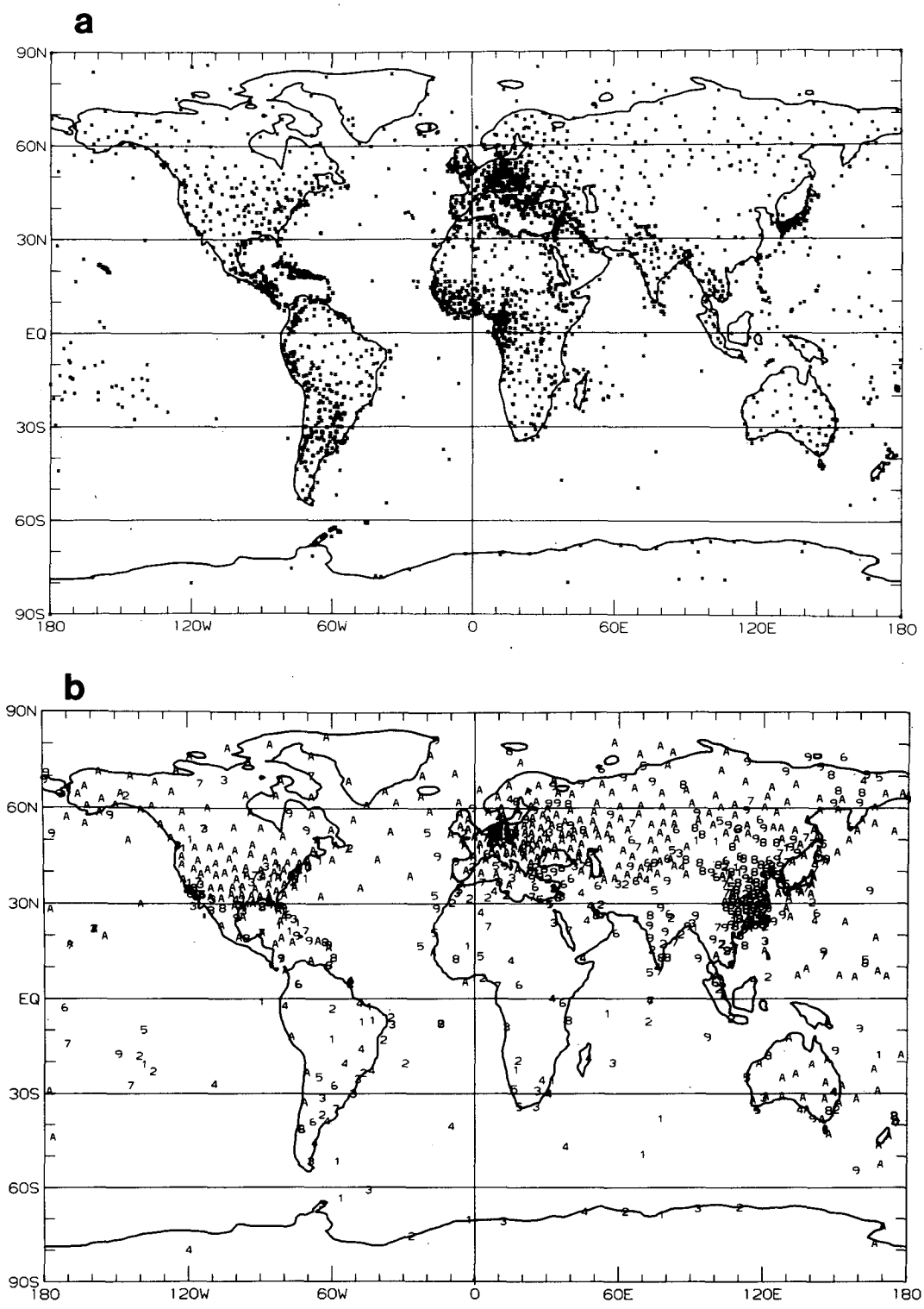

FIG. 2. (a) The geographic distribution of surface stations reporting surface pressure during the 15-year period, May 1958–April 1973. (b) The geographic distribution of upper air stations reporting the height of the 850 mb pressure level during the 10-year period May 1963–April 1973. Plotted is the number of years of observations used in the monthly analysis of the 850 mb height fields, where *A* (=10) indicates the maximum number of years with good data.

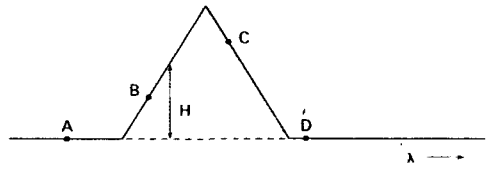

FIG. 3. A hypothetical east–west topographic feature, used in the text to discuss possible errors due to the grid point distribution. A, B, C and D are grid points.

lem is further accentuated in mountainous areas with sparse data, such as over central Asia and over the northern Andes during 1900–58.

The seasonal mountain torque results are apparently more reliable. Latitude-dependent results are shown in Figs. 4a and 5a for the seasonal deviations from the annual mean averaged over the Northern Hemisphere winter (December, January, February) and Northern Hemisphere summer (June, July, August). Both the 1900–58 and 1958–73 results are shown. The mountain torque values presented in Figs. 4a and 5a represent T_M computed from (5) and integrated over 5° wide latitude belts. Units are in Hadleys per 5° latitude (1 Hadley = 10^{18} kg m^2 s^{-2}). A positive value denotes an eastward torque on the atmosphere.

The good agreement between the 1900–58 and the 1958–73 results in Figs. 4a and 5a suggests that the

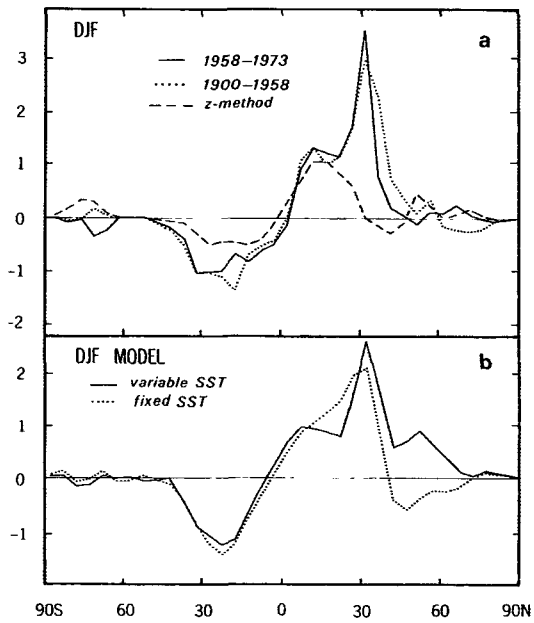

FIG. 4. Latitudinal profiles of the mountain torque in Hadleys (10^{18} kg m^2 s^{-2}) per 5° latitude, averaged over the Northern Hemisphere winter (December, January, February). *The latitude-dependent annual mean has been removed.* (a) Results inferred from real data: two estimates from surface pressure data over different time periods, and an estimate from isobaric height data. (b) Results from two versions of a GFDL general circulation model of the atmosphere, computed using the simulated surface pressure.

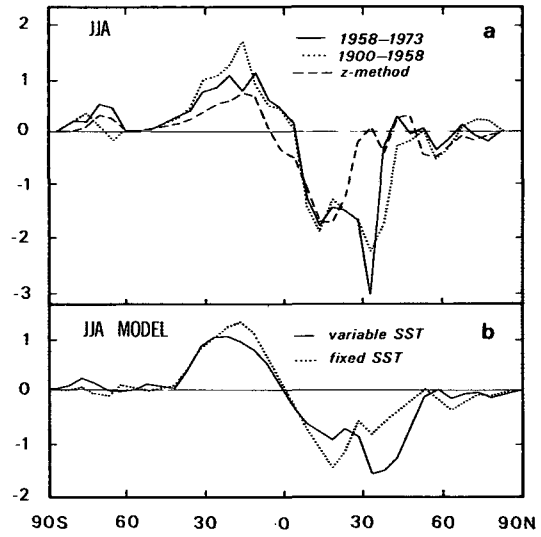

FIG. 5. Latitudinal profiles of the mountain torque in Hadleys per 5° latitude, averaged over the Northern Hemisphere summer (June, July, August). *The latitude-dependent annual mean has been removed.* (a) Results from real data. (b) Results from the GFDL models.

effects of discrete grid point sampling are not as serious in the seasonal results as in the annual-mean results. This is consistent with the fact that elevation-dependent terms are nearly constant in time, and so are relatively more important in determining the annual-mean pressure field than in determining the seasonally varying field.

There is, however, some uncertainty due to uneven station coverage, particularly over central Asia where there is a sizeable region with large topographic gradients but few reporting stations. In fact, additional Chinese data for a portion of the missing region (received in the final stages of revision of this paper) suggest that the mountain torque estimates between 25°N and 40°N may be too large.

There is an alternative method for computing the mountain torque used by Newton (1971a) and Oort and Bowman (1974). Let $z(p, \phi, \lambda)$ represent the elevation above sea level of the pressure level p at the point (ϕ, λ). Then $H(\phi, \lambda) = z(p_s, \phi, \lambda)$ where p_s is the surface pressure at (ϕ, λ), and (2) is equivalent to

$$T_M = \frac{-a^2\pi}{180}\cos\phi \int_0^{2\pi} d\lambda \int_0^{p_s} \left(\frac{\partial z}{\partial \lambda}\right) dp. \qquad (7)$$

To derive (7) from (3), we used the fact that

$$\frac{\partial}{\partial \lambda}\left(\int_0^{p_s} z dp\right) = \int_0^{p_s} \left(\frac{\partial z}{\partial \lambda}\right) dp + H\frac{\partial p_s}{\partial \lambda}.$$

We have used (7) to compute the annual-mean and seasonal mountain torques from monthly, global rawinsonde observations of the z-field for 1963–73, from Oort (1983). These data consist of observed heights of

11 different pressure levels in the atmosphere (1000, 950, 900, 850, 700, 500, 400, 300, 200, 100, and 50 mb) taken at about 600 stations. As an example, the locations of those stations reporting 850 mb data are shown in Fig. 2b. The data were analyzed and interpolated to a 5° longitude by 2.5° latitude grid, using the same interpolation technique as applied above to the surface pressure data.

The discrete form of equation (7) used here is

$$T_M = \frac{-a^2\pi}{180}\cos\phi \sum_{i,j} \frac{1}{2}(\Delta p)^j s_i^j (z_{i+1}^j - z_{i-1}^j), \quad (8)$$

where z_i^j is the z-field at the longitudinal grid point i and pressure level j, s_i^j is the tag array defined by $s_i^j = 1$ if pressure level j lies above the local topography, and $s_i^j = 0$ otherwise, and $(\Delta p)^j$ is one half the pressure difference between the $j+1$ and $j-1$ pressure levels. The time independent array, s_i^j, was smoothed to have approximately the same horizontal resolution as the interpolated z-field data.

An apparent advantage of the surface pressure results is that there are roughly four times as many stations reporting surface pressure as there are stations in the rawinsonde network. On the other hand, the stations reporting pressure are grouped closely together and so supply effectively redundant information. In fact, in many areas, such as central Asia, the horizontal resolution of the rawinsonde network may be as good as that of the surface pressure data set. A problem common to both methods is that because of the grid point resolution both techniques are incapable of representing the torque due to small scale topography: less than 5° in longitude and 2.5° in latitude.

One advantage of the z-field method is that it is probably less sensitive to the grid point distribution errors which plague the annual mean surface pressure results. The latitude dependent annual mean results computed from the z-field data are given in Fig. 6a. Also shown is the annual-mean mountain torque from Newton (1971a), who used isobaric height data in a similar fashion together with a hand-interpolation scheme to find T_M. Differences are most pronounced at low latitudes. Otherwise, the dominant features in these results are the strong westward torques on the atmosphere in midlatitudes, presumably associated with the midlatitude westerlies. It should be emphasized that a simple direct relation between wind direction/speed and mountain torque is by no means assured (see, e.g., White, 1949).

Latitude-dependent seasonal departures from the annual mean, computed from the z-field data, are also shown in Figs. 4a and 5a for the Northern Hemisphere winter and the Northern Hemisphere summer, respectively. The seasonal departures are qualitatively similar to the corresponding results computed from surface pressure data. Particularly evident are the apparent effects of the trade winds at low latitudes, which

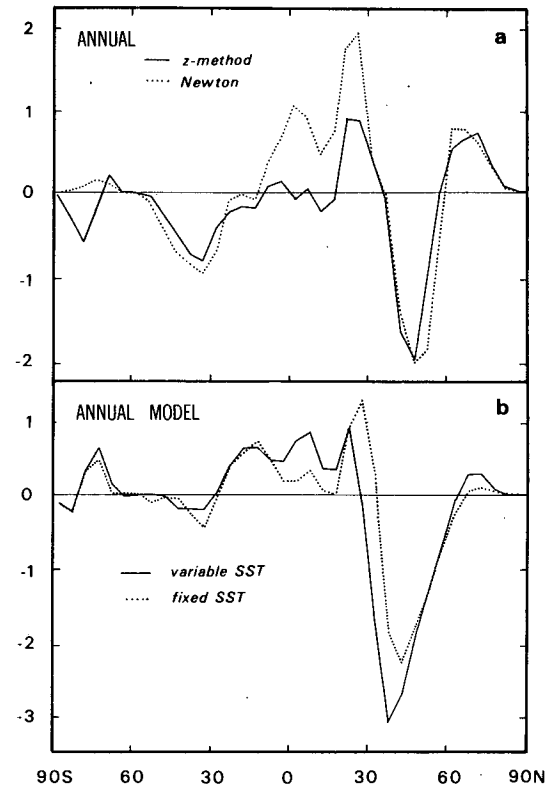

FIG. 6. Latitudinal profiles of the annual-mean mountain torque, in Hadleys per 5° latitude. (a) Results from isobaric height data and from Newton (1971a). (b) Results from the GFDL models.

seem to lead to strong eastward torques on the atmosphere during winter. In general, the seasonal variations computed from the z-field data are smaller than those from the surface pressure data. This is particularly true at latitudes near 30°N, where the surface pressure results show pronounced deviations from the annual mean in both summer and winter, but where the z-field results show little seasonal variation.

The latitude-dependent seasonal departures from both methods are further integrated over latitude to give monthly hemispheric and global values. These are shown in Figs. 7a, 8a and 9a. The agreement among the two sets of surface pressure and z-field analyses is encouraging. In the Northern Hemisphere there is an eastward torque on the atmosphere during the Northern Hemisphere winter, and a westward torque during the Northern Hemisphere summer. The Southern Hemisphere results are roughly 180° out of phase and have smaller amplitude (which would be expected because of more pronounced topography in the Northern than in the Southern Hemisphere). The global results are not as well determined, due to partial cancellation of the contributions from the two hemispheres, but appear to be roughly in phase with the variation of the torque in the Northern Hemisphere.

We have also computed the mountain torque using

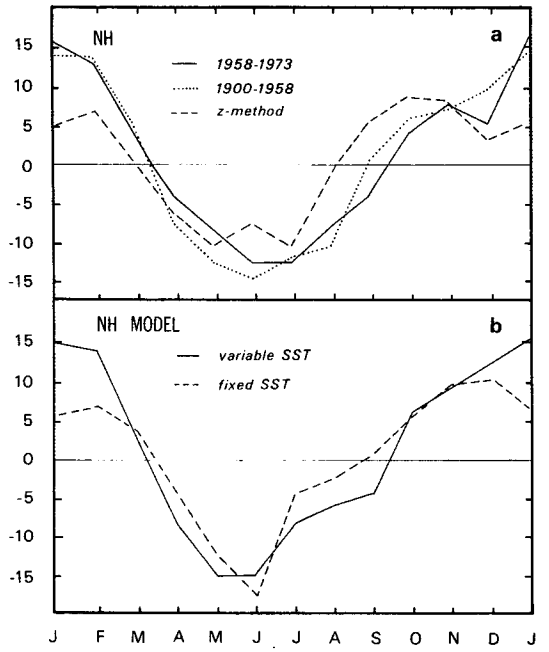

FIG. 7. Monthly mountain torques in Hadleys, integrated over the Northern Hemisphere. *The annual mean has been removed.* (a) Results from real data. (b) Results from the GFDL models.

surface pressure results from two GFDL general circulation models. These models have been reasonably successful in representing the seasonal behavior of the atmospheric circulation. Detailed descriptions of these models and their results can be found in Manabe *et al.* (1979), Manabe and Stouffer (1980), and Manabe and Hahn (1981). The specific models used here are (1) an atmospheric general circulation model with prescribed, seasonally varying sea surface temperatures (fixed SST model) described by Manabe and Hahn (1981), and (2) an atmospheric general circulation

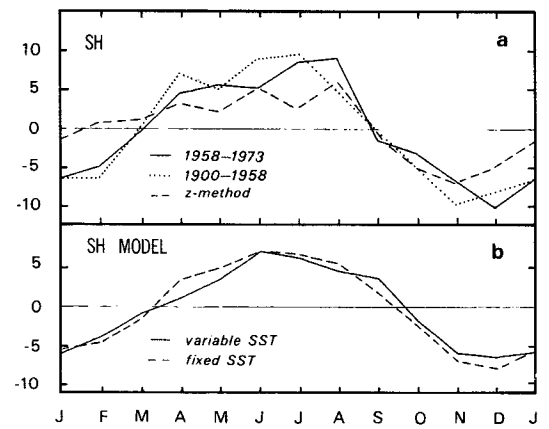

FIG. 8. Monthly mountain torques in Hadleys, integrated over the Southern Hemisphere. *The annual mean has been removed.* (a) Results from real data. (b) Results from the GFDL models.

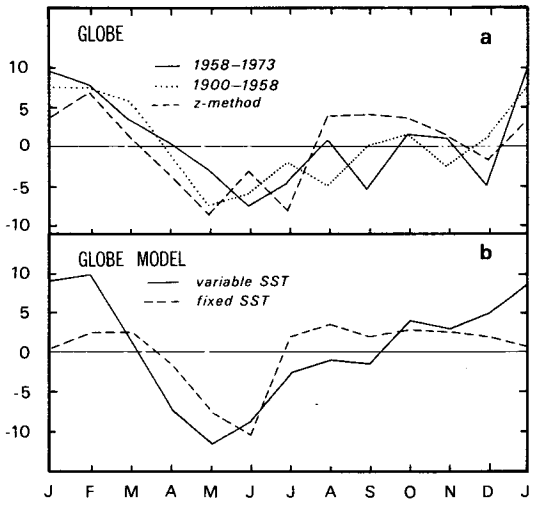

FIG. 9. Monthly mountain torques in Hadleys, integrated over the globe. *The annual mean has been removed.* (a) Results from real data. (b) Results from the GFDL models.

model coupled with a mixed-layer ocean (variable SST model) described by Manabe and Stouffer (1980). The fixed SST model produced results that are probably more representative of the real atmosphere, but the output from that model did not include explicit results for the friction stress. Therefore, the friction stress from the fixed SST model will not be discussed in Section 3.

The seasonal data from the fixed and variable SST models were constructed by averaging over 15 and 4 model years, respectively, after equilibrium was reached in the model integrations. The computed surface pressures are used in (5) to compute annual mean and seasonal departure values for the model mountain torques. Latitudinal profiles are shown in Figs. 4b, 5b (departures from the mean for the Northern Hemisphere winter and summer) and 6b (annual mean). Hemispheric and global seasonal departures are given in Figs. 7b, 8b and 9b. In all cases, results are qualitatively similar to the results from real data. The implication is that the models do a respectable job in reproducing the seasonal mountain torque.

3. Friction torque

The friction torque on the atmosphere is the torque due to viscous drag as the winds blow over the earth's surface. The zonal component of this torque, per unit area, at any point **r** on the earth's surface is

$$\hat{\Omega} \cdot (\mathbf{r} \times \tau) = r \cos\phi \tau_\lambda,$$

where τ is the frictional surface traction on the earth (at **r**) due to the atmosphere, and τ_λ is the eastward component of τ. Then, the zonal friction torque integrated over a 1° latitude wide belt is given by

$$T_F = \frac{-a^3\pi}{180}\cos^2\phi \int_0^{2\pi} \tau_\lambda d\lambda. \quad (9)$$

The friction stress over the ocean is usually parameterized as (see, e.g., Bunker, 1976)

$$\tau_\lambda = \rho c_d |\mathbf{v}| u, \quad (10)$$

where $\mathbf{v}$ is the surface wind velocity vector, u is the eastward component of $\mathbf{v}$, ρ is the surface atmospheric density, and c_d is an empirically determined, reasonably well understood dimensionless coefficient. Hellerman and Rosenstein (1983) have constructed a seasonally averaged data set over the world ocean, using all available daily observations of surface wind velocities from the 20th century. They used $\rho = 1.2$ kg m^{-3} and modeled c_d as dependent on $|\mathbf{v}|$ and on stability after Bunker (1976). The data are presented on a 2° × 2° grid over the oceans. We have used these results for τ_λ in (9) to find the seasonal contributions to T_F from friction stress over the oceans.

Unfortunately, friction stress over land, which is also needed to complete the calculation of T_F, is not well understood. Therefore, we have estimated the friction stress over land by assuming that the zonal stress per unit area averaged over an entire latitudinal belt is equal to the zonal stress per unit area averaged over only the ocean at that latitude. The physical basis for this assumption is that while the surface roughness tends to be greater over land than over oceans, the surface winds tend to be weaker over land leading to similar stress values over land and oceans (Kung, 1968; Smagorinsky, 1960). This procedure is implemented numerically by integrating (9) over only the oceans using Hellerman and Rosenstein's data for τ_λ, and then multiplying the result by the ratio of total surface area to oceanic area at that latitude. Although this assumption about the average friction stress over land is consistent with results from the GFDL general circulation model (see below), it is possibly the weakest point in our friction torque estimates. Problems are particularly apt to occur in the Asian monsoon belt between 0 and 30°N during summer (see the discussion of the model results, below).

Latitude-dependent results for T_F, averaged over 5° latitude belts, are shown in Fig. 10 for the Northern Hemisphere winter and summer. The annual mean has not been removed. A comparison with Figs. 4, 5 and 6 confirms the conclusion from earlier studies (e.g., Newton, 1971a) and shows that at many latitudes the friction torque is as much as three to four times larger than the mountain torque. An exception may occur near 30°N where the mountain torque is found to be large from both the surface pressure method and the model data, whereas the friction torque almost vanishes. Also shown in Fig. 10 are corresponding results for T_F integrated only over the ocean areas. The difference between the solid and dotted curves in Fig. 10 represents the estimated contribution to T_F from the friction stress over the continents. However, because of the ad hoc way in which friction stress over land is estimated, the results for the continents should not be taken too seriously.

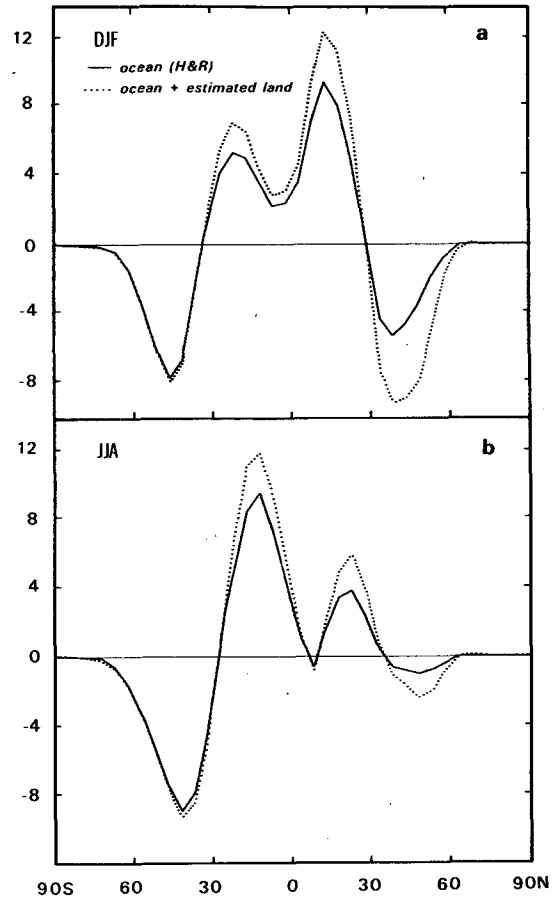

FIG. 10. Latitudinal profiles of the friction torque in Hadleys per 5° latitude, estimated from the oceanic stress data of Hellerman and Rosenstein (1983). The annual mean has *not* been removed. The solid line is the torque over only the ocean. The dashed line includes an estimate for the torque over land, obtained by extending the oceanic stress data assuming equal stress over land and oceans (see text). (a) Results for the Northern Hemisphere winter. (b) Results for the Northern Hemisphere summer.

These latitudinal profiles were further integrated with respect to latitude to give hemispheric and global estimates. However these results are not shown here because they show little annual or semiannual variations and appear unreliable in general. The problem is the large cancellation when one integrates over a hemisphere, so that the final integrals are more sensitive to errors (such as inadequate surface wind data and the assumption about the friction stress over land) than the latitude-dependent results shown in Fig. 10.

Friction stress results from the GFDL variable SST general circulation model are also used in (9) to find model estimates for the friction torque. Latitudinal profiles are given in Fig. 11. (The results from the fixed

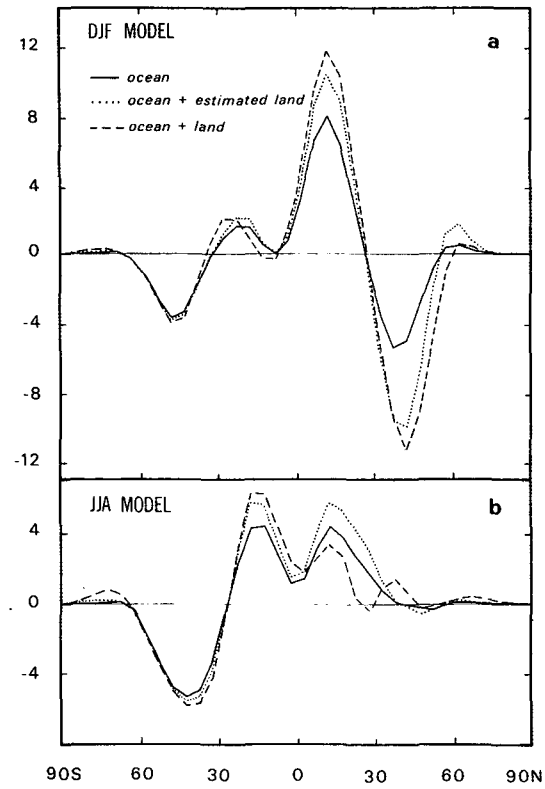

FIG. 11. Latitudinal profiles of the friction torque in Hadleys per 5° latitude, estimated from the GFDL variable SST model. The annual mean has *not* been removed. The solid line is the torque over only the ocean. The dashed line is the torque over both land and ocean. The dotted line is the torque over the ocean plus an estimate for the torque over land, obtained by extending the oceanic stress (see text). (a) Results for the Northern Hemisphere winter. (b) Results for the Northern Hemisphere summer.

SST model are not shown because surface windstress data were not readily available.) Shown here are results for T_F integrated over the oceans only as well as over oceans plus land. In addition, we show the model estimate for T_F over the entire latitude belt, based on ocean stress data extended over land using the same assumption as adopted above for real data: i.e., the average zonal stress over land at any latitude equals the average stress over the ocean at that latitude.

One implication from Fig. 11 is that for the model the seemingly ad hoc extension of ocean-averaged stress to land gives generally good results, except for low latitudes in the Northern Hemisphere during the summer. In the GFDL model, friction stress over both the ocean and the continents is parameterized in terms of surface velocity as shown in (10). The dimensionless parameter c_d is chosen to be independent of velocity, with $c_d = 0.001$ over the ocean and $c_d = 0.003$ over land. These c_d values were chosen to be somewhat smaller than the observed ones because the reference level for specifying the surface winds in the models is at about 70 m height rather than at about 10 m height, the usual anemometer level. Evidently the greater viscous coupling over land acts to decrease the surface wind speeds in such a way that the zonal stress over land and oceans remains the same. A similar conclusion was found by Smagorinsky (1960), using a predecessor of the present GFDL model. He found that a large numerical change in the c_d parameter had little effect on the surface stress. Although these results are encouraging in their support of the similarity between real continental and oceanic stresses, they are by no means conclusive.

One place of poor agreement between the exact and the estimated ocean-plus-land results shown in Fig. 11 is in the Northern Hemisphere summer at latitudes between 0 and 30°N. This is apparently due to the model simulation of the summer monsoon over southern Asia. The local surface winds associated with the monsoon are eastward, and in the model these winds are concentrated mainly over land. Since the zonally averaged winds over the ocean are westward, the resulting friction stress cannot be accounted for by simply extending the averaged oceanic stress over the continents. A similar bias probably also occurs in the estimates derived from real data, shown in Fig. 10b.

On the other hand, the variable SST model does not do a good job in reproducing the observed summer monsoon circulation over southeast Asia. The unrealistic trade winds over the Indian Ocean are connected with the fact that the simulated Intertropical Convergence Zone is too far south. This, in turn, is caused by the model-simulated SST in the Southern Hemisphere, which are several degrees too high, while they are realistic in the Northern Hemisphere (Manabe, personal communication). As a result, the model friction torque in Fig. 11b between 0 and 30°N is probably incorrect. Another discrepancy with observations is that the model estimates of the friction torque in the Southern Hemisphere are generally too small. The explanation is simply that the surface winds in the model are too weak in the Southern Hemisphere.

Hemispheric and global results from the variable SST model are shown in Fig. 12. As mentioned before, the hemispheric and global integrals of the observed friction torques are too unreliable to be presented here. We will argue in Section 4 that the total, global torque is well represented by the model data. Since the global mountain torque estimated from the model is in fair agreement with the corresponding estimates from real data (Fig. 9), the implication is that despite the apparent problems with the latitude-dependent friction torque derived from the model, the global estimates of the friction torque may be reasonably reliable.

4. Total torque

Surface torques act to transfer angular momentum between the atmosphere and the earth. As a result, if the flux and time rate of change of atmospheric angular

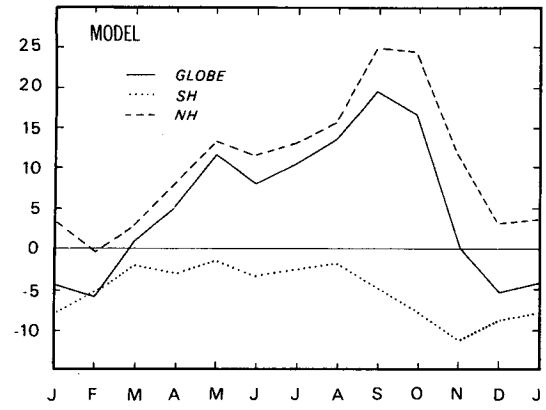

FIG. 12. Monthly friction torques in Hadleys, estimated from the GFDL variable SST model and integrated over the Northern and Southern Hemispheres and over the globe. The annual mean has *not* been removed.

momentum could be inferred from meteorological data, the total external torque could be estimated.

Let V be an atmospheric volume which is bounded below by the earth and above by the "top" of the atmosphere. Then, the time rate of change of angular momentum in V must equal the flux of angular momentum into V through its side boundaries plus the total external torque on V. In general, that torque will include the mountain and friction torques from the solid earth and oceans, plus pressure and viscous torques from the atmosphere surrounding V. If the volume, V, is a uniform belt of constant latitude around the earth, the zonal pressure torque from the surrounding atmosphere will vanish identically. Furthermore, since shear stresses within the atmosphere are small, the viscous torque from the surrounding atmosphere can be neglected. So, in this case

$$\frac{\partial}{\partial t}\int_V MdV = \int_{S_V} M\hat{\mathbf{n}}\cdot\mathbf{v}dS + T, \qquad (11)$$

where M is the zonal angular momentum of the atmosphere, S_V represents the latitudinal walls of the volume V, $\hat{\mathbf{n}}$ is the normal to S_V ($\hat{\mathbf{n}}$ is directed into V), $\mathbf{v}$ is the wind velocity, and

$$T = \int_{\Delta\phi} (T_F + T_M)d\phi$$

is the sum of the mountain torque and the friction torque acting on V from the underlying earth ($\Delta\phi$ is the width of the latitude belt, V). If V has a width of 5° in latitude, T can be expressed in Hadley units per 5° latitude, and the results inferred from (11) can be compared directly with the torque estimates computed above.

We used monthly atmospheric angular momentum data, as described by Oort and Peixoto (1983), to estimate seasonal results for T integrated over 5° latitude belts. The results are shown by the solid lines in Fig. 13 for the Northern Hemisphere winter and summer. The annual mean has not been removed. In general, for 5° latitude belts the flux term $\int_S M\hat{\mathbf{n}}\cdot\mathbf{v}dS$ in (11) is considerably larger than the volume integral $(\partial/\partial t)\int_V MdV$. The flux becomes relatively less important for wider latitude belts. In fact, when integrated over the entire globe the flux term vanishes identically.

To find the latitudinal profiles shown in Fig. 13, we considered only the relative angular momentum M_r (the angular momentum due to winds—see the introduction). We did not include the effects of horizontal or vertical shifts in atmospheric mass, which cause changes in the Ω-angular momentum. These effects are expected to be small (see, e.g., Newton, 1971b).

Also shown in Fig. 13 is the sum of the friction torque, computed from Hellerman and Rosenstein's (1983) data and extended over land as described in Section 3, and the mountain torque, computed from the z-field data as described in Section 2. The annual mean has not been removed from these results. The decision to use the z-field mountain torque in this case, rather than the surface pressure results, was based on the presumably greater reliability of the z-field data in estimating the annual mean. However, in any case, the total torque at most latitudes is dominated by the

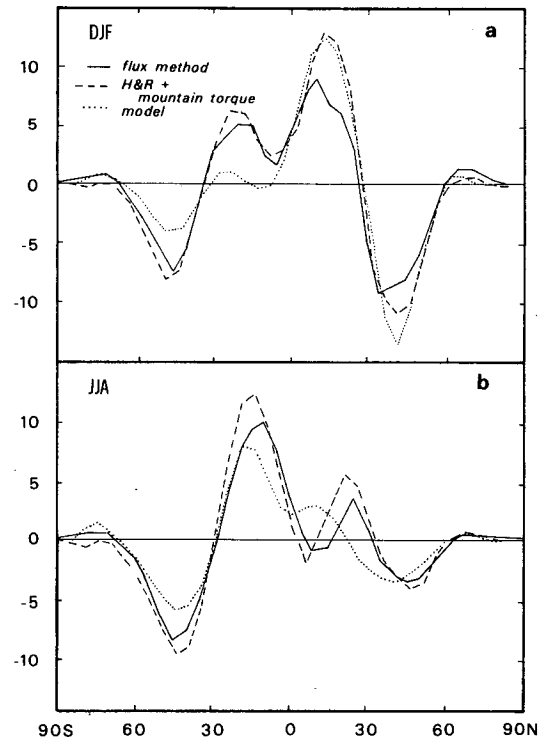

FIG. 13. Latitudinal profiles of the total torque in Hadleys per 5° latitude. The annual mean has *not* been removed. Results are given for the angular momentum flux method, for the sum of the estimated friction and mountain torques, and for the GFDL variable SST model. (a) Northern Hemisphere winter. (b) Northern Hemisphere summer.

friction torque, and using, for example, the mountain torque values based on the 1958–1973 surface pressures does not substantially change the results shown in Fig. 13. Also shown in Fig. 13 are estimates of the total torque computed from the GFDL variable SST general circulation model.

There is reasonably good qualitative agreement in Fig. 13 between the results from the angular momentum flux method and the total observed torque. In both cases the opposing effects of the trade winds and the midlatitude westerlies are evident.

As argued in Section 3, the differences between these estimates and the results inferred from the variable SST model are probably mostly due to inadequacies in the model, especially in the Southern Hemisphere. The model simulated winds in the Southern Hemisphere are too weak, leading to an underestimate of the surface stresses throughout the year. Furthermore, the model monsoon westerlies seem to be too far north over the Asian continent, producing the positive anomaly centered near 10°N and the negative anomaly near 30°N in Fig. 13b.

The latitudinal profiles for the total torque estimated from the angular momentum data and from the variable SST model, are summed over latitude to give hemispheric and global estimates for the total seasonal torque. Results are shown in Fig. 14. In this case, the global estimates *do* include the effects of Ω-angular momentum caused by horizontal mass redistributions within the atmosphere. These effects on the global torque are 10% or less of the results computed from the relative angular momentum alone. Estimates derived from the observed friction and mountain torques are not presented here, since, as described in Section 3, the hemispheric and global friction torques are probably not well determined by the data.

There is fairly good qualitative agreement between the flux method and the model results shown in Fig. 14. The model predicts an eastward torque on the atmosphere in the Northern Hemisphere that is apparently too large during August through November, and a westward torque in the Southern Hemisphere that is too large during October through January. However, the model does reproduce the general seasonal trends in both hemispheres.

A completely independent estimate of the seasonal global torque on the atmosphere can be inferred from astrometric observations of variations in the earth's rotation rate. Hide *et al.* (1980) and Rosen and Salstein (1983) have been successful in explaining short-period variations in the earth's rotation rate in terms of an exchange of angular momentum with the atmosphere. Seasonal changes in the rotation rate, which produce corresponding changes in the length of day (lod), are caused not only by the seasonal exchange of angular momentum between the solid earth and the atmosphere, but also by the tidal forces from the sun and moon (see, e.g., Lambeck, 1980, for a complete review).

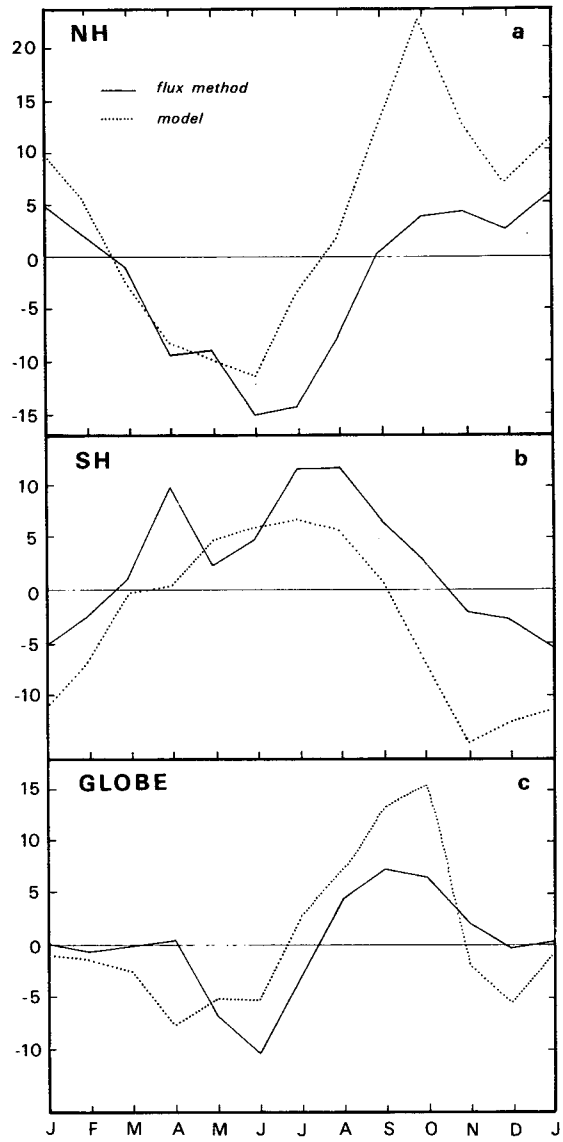

FIG. 14. Monthly values of the total torque in Hadleys, integrated over: (a) the Northern Hemisphere; (b) the Southern Hemisphere; (c) the globe. The annual mean has *not* been removed. Results are given for the angular momentum flux method and for the GFDL variable SST model.

The tidal variations are important but are well understood (see, e.g., Merriam, 1982). The effects of ocean currents are not well known but are apparently small (see Lambeck and Hopgood, 1981, Wahr, 1983).

The most evident and best determined variations in the lod occur at the annual and semiannual periods. We have taken observed annual and semiannual lod amplitudes from Lambeck and Hopgood (1981) and subtracted the estimated effects of tides (using values from Lambeck and Hopgood) and ocean currents (using the effects of the circumpolar current from Lambeck and Hopgood and noting from Wahr, 1983, that

the effects of other currents are probably negligible). The results should directly reflect the transfer of angular momentum between the earth and the atmosphere at these periods.

The implied annual-plus-semiannual torques on the atmosphere are shown by the solid curves in Figs. 15a and 15b. Also shown in Fig. 15a are the total annual-plus-semiannual torques estimated from the global rate of change of relative angular momentum in the atmosphere. These results were obtained by extracting the annual and semiannual components from the results shown in Fig. 14c.

The good agreement in Fig. 15a between the estimates inferred from angular momentum data and the results derived from observations of the earth's rotation rate, has been discussed by, e.g., Lambeck and Hopgood (1981), and Wahr (1983). The slight disagreement between the two curves in Fig. 15a is probably mostly due to the fact that the angular momentum observations do not adequately sample the winds near the top of the atmosphere. Using data from Belmont *et al.* (1974), Lambeck and Hopgood (1981) estimated that stratospheric winds affect the global results by up to 10–20% at the annual and semiannual frequencies.

The annual-plus-semiannual global torque inferred from the lod observations is compared in Fig. 15b with corresponding results predicted from both the variable SST and the fixed SST general circulation models. Since the fixed SST model output did not include results for the surface stress, the total torque for that model had to be computed using the first term in (11), together with model zonal wind data. To be consistent, the variable SST estimates in Fig. 15b were also computed from the zonal wind data.

If the models conserved angular momentum, then the model results shown in Fig. 15b should, in principle, be identical to the corresponding results inferred directly from the simulated surface torque. For the variable SST model, global estimates from the torque and angular momentum methods are in good, but not perfect, agreement. The annual-plus-semiannual components agree closely in phase but differ in amplitude by up to two Hadleys (usually less) at any given month. This difference does not necessarily imply that the model does not conserve angular momentum, although this possibility cannot be ruled out. Instead, it may be a consequence of the fact that we have computed the torques from model data that have been interpolated and averaged at time and space resolutions different from those used within the model itself.

In any case, the differences between the torque and angular momentum results are small enough that our interpretation of Fig. 15b is not affected. That is, results from both models agree well with the lod observations. The fixed SST results show a slightly better phase agreement, while the amplitude of the seasonal variation in both sets of model estimates seems somewhat too large. But the agreement is good enough to suggest that the global seasonal friction torque, estimated from the variable SST model and shown in Fig. 12, may be reasonably accurate. This, of course, has no direct implications for the latitude-dependent or hemispheric torques inferred from the model.

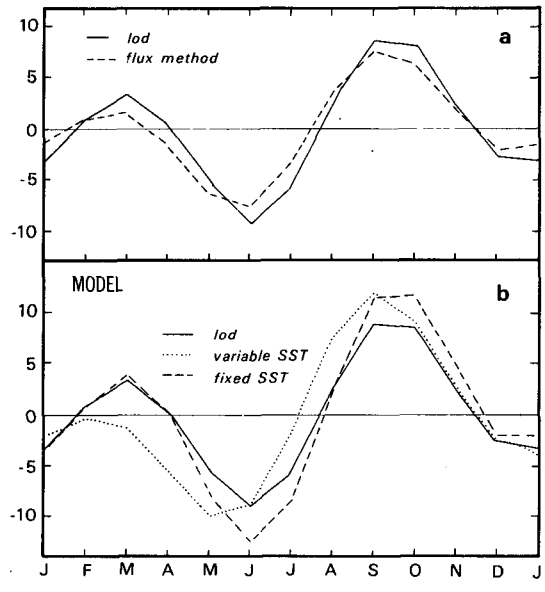

FIG. 15. Monthly values of the total torque in Hadleys, integrated over the globe. Only the annual and semiannual components are included. The solid line represents the values inferred from astronomical observations of the length of day (lod). The lod values are compared with: (a) results inferred from the angular momentum flux method; (b) results from the GFDL models.

5. Summary

We have used a number of independent data sets to construct estimates for the seasonal, zonal surface torques. The mountain torque was computed both from surface pressure data and from isobaric height data. The friction torque was estimated using oceanic surface stress data from Hellerman and Rosenstein (1983) and extending the results over land by assuming equal stress over land and oceans. The sum of the estimated friction and mountain torques was compared with results for the total torque obtained from atmospheric angular momentum data. Finally, the total torque integrated over all latitudes was compared with astrometric observations of the seasonal variation in the earth's rotation rate. These intercomparisons helped to identify those features in the results that might or might not be meaningful.

Results for the latitude-dependent mountain torque suggest that the seasonal departures from the annual mean are reasonably well determined by both the surface pressure and the isobaric height data, except at latitudes near 30°N, where the two estimates give different results. The problems near 30°N are associated with the large topographic gradients in the Himalaya's

and could conceivably be resolved by using additional surface pressure data from Central Asia. Otherwise,the results at low latitudes are consistent with the direction and strength of the trade winds.

The annual-mean mountain torque is not as well determined. The results computed from surface pressure data are not reliable, due to problems associated with the grid point distribution and the inadequate data coverage over many mountainous areas. The most conspicuous features in the annual-mean results derived from isobaric height data are the pronounced westward torques at midlatitudes associated with the midlatitude westerlies. It is interesting that the effects of these winds are not evident in the seasonal departures from the annual mean.

Results for the hemispheric-averaged mountain torque are in reasonably good agreement. The torque on the atmosphere in the Northern Hemisphere is westward during the Northern Hemisphere summer, and eastward during the winter, in agreement with the increase in strength of the trade winds during winter. Results for the Southern Hemisphere are 180° out of phase with those for the Northern Hemisphere, and have smaller amplitude. The global estimates show more scatter, but are approximately in phase with the Northern Hemisphere results.

It is harder to directly assess the results for the friction torque given here, since we used only one independent data set over the oceans and no data at all over land. Results from the GDL general circulation model suggest, though do not prove, that the zonal extrapolation of ocean stress data to land may be adequate, except possibly for the Asian monsoon region during summer. Nevertheless, this is probably the major source of uncertainty in the friction torque results.

Indirect support for the friction torque estimates can, however, be obtained by comparing the sum of the mountain and friction torques with the total torque as determined from atmospheric angular momentum data. Since at most latitudes the friction torque is much larger than the mountain torque, and since the mountain torque is probably well determined anyway, this comparison can be interpreted as a constraint on the friction torque estimate. Although the computed friction-plus-mountain torque is generally slightly larger than the total torque estimated from angular momentum data, the overall qualitative agreement is good. Particularly evident are the effects of the easterly trade winds at low latitudes and the midlatitude westerlies.

Hemispheric and global torques are, however, not well determined by the friction stress data. These results do not agree at all well with either the angular momentum data or with astrometric observations of the length of day. On the other hand, the global torque estimated from the time rate of change of atmospheric angular momentum is probably reliable, since it does agree well with the length of day observations. Both the global and the hemispheric total torque values derived from angular momentum data are in phase with the corresponding results for the mountain torque alone. That is, the total torque in the Northern Hemisphere is westward in the Northern Hemisphere summer and eastward in the winter, the total torque in the Southern Hemisphere is 180° out of phase with the Northern Hemisphere torque, and the global torque is roughly in phase with the torque in the Northern Hemisphere.

We also compared all of these surface torque estimates with corresponding results simulated by two versions of the GFDL general circulation model of the atmosphere. Agreement was, in general, good. Some of the most important differences could be explained in terms of known deficiencies in the model.

Acknowledgments. We are grateful to Syukuro Manabe, Chester Newton, Ray Pierrehumbert and Gareth Williams for helpful discussions and for their comments on the manuscript. We thank Kathy Bilous for typing the manuscript and Belle Koblentz for help in preparing the figures. Financial support was provided by the GFDL Visiting Scientist Program (NOAA Grant 04-7-022-44017), by the National Aeronautics and Space Administration (NASA Grant NAS5-27341) and by the National Science Foundation (NSF Grant EAR-8115903).

REFERENCES

Belmont, A. D., D. G. Dartt and G. D. Nastrom, 1974: Periodic variations in stratosphere zonal wind from 20 to 65 km, at 80°N to 70°S. *Quart. J. Roy. Meteor. Soc.*, **100**, 203–211.

Bunker, A. F., 1976: Computations of surface energy flux and annual air–sea interaction cycles of North Atlantic Ocean. *Mon. Wea. Rev.*, **104**, 1122–1140.

Hellerman, S., 1967: An updated estimate of the wind stress on the world ocean. *Mon. Wea. Rev.*, **95**, 607–626 (see corrected tables in **96**, 62–74).

——, and M. Rosenstein, 1983: Normal monthly wind stress over the world ocean with error estimates. *J. Phys. Oceanogr.*, **13**, 1093–1104.

Hidaka, K., 1958: Computation of wind stresses over the oceans. *Records Oceanogr. Works Japan*, **4**, 77–123.

Hide, R., N. T. Birch, L. V. Morrison, D. J. Shea and A. A. White, 1980: Atmospheric angular momentum fluctuations and changes in the length of the day. *Nature*, **286**, 114–117.

Kung, E. C., 1968: On the momentum exchange between the atmosphere and earth over the Northern Hemisphere. *Mon. Wea. Rev.*, **96**, 337–341.

Lambeck, K., 1980: *The Earth's Variable Rotation: Geophysical Causes and Consequences.* Cambridge University Press, 449 pp.

——, and P. Hopgood, 1981: The Earth's rotation and atmospheric circulation from 1963 to 1973. *Geophys. J. Roy. Astron. Soc.*, **64**, 67–89.

Lorenz, E. N., 1967: *The Nature and Theory of the General Circulation of the Atmosphere.* WMO, 161 pp.

Manabe, S., and R. J. Stouffer, 1980: Sensitivity of a global climate model to an increase of CO_2 concentration in the atmosphere. *J. Geophys. Res.*, **85**, 5529–5554.

——, and D. G. Hahn, 1981: Simulation of atmospheric variability. *Mon. Wea. Rev.*, **109**, 2260–2286.

——, ——, and J. L. Holloway, 1979: Climate simulation with

GFDL spectral models of the atmosphere. GARP Publ. Ser. 22, WMO, 41–94.

Merriam, J. B., 1982: A comparison of recent theoretical results on the short-period terms in the length of day. *Geophys. J. Roy. Astron. Soc.*, **69,** 837–840.

Newell, R. E., J. W. Kidson, D. G. Vincent and G. J. Boer, 1972: *The General Circulation of the Tropical Atmosphere and Interactions with Extratropical Latitudes.* Vol. 1, The MIT Press, 258 pp.

Newton, C. W., 1971a: Mountain torques in the global angular momentum balance. *J. Atmos. Sci.*, **28,** 623–628.

——, 1971b: Global angular momentum balance: Earth torques and atmospheric fluxes. *J. Atmos. Sci.*, **28,** 1329–1341.

Oort, A. H., 1983: Global atmospheric circulation statistics, 1958–1973. NOAA Prof. Pap. 14, 180 pp. + 47 microfiche.

——, and E. M. Rasmusson, 1971: Atmospheric circulation statistics. NOAA Prof. Pap. 5, 323 pp.

——, and D. Bowman II, 1974: A study of the mountain torque and its interannual variations in the Northern Hemisphere. *J. Atmos. Sci.*, **31,** 1974–1982.

——, and J. P. Peixoto, 1983: Global angular momentum and energy balance requirements from observations. *Advances in Geophysics,* Vol. 25, Academic Press, 355–490.

Priestley, C. H. B., 1951: A survey of the stress between the ocean and the atmosphere. *Aust. J. Sci. Res.*, **A4,** 315–328.

Rosen, R. D., and D. A. Salstein, 1983: Variations in atmospheric angular momentum on global and regional scales and the length of the day. *J. Geophys. Res.*, **88,** 5451–5470.

——, —— and J. P. Peixoto, 1979: Variability in the annual fields of large-scale atmospheric water vapor transport. *Mon. Wea. Rev.*, **107,** 26–37.

Smagorinsky, J., 1960: General circulation experiments with the primitive equations—as a function of the parameters. Extended Abstracts, IUGG, General Assembly, Helsinki, 1960, 55–56. [Available from GFDL/NOAA, Princeton University.]

Smith, R. B., 1978: A measurement of mountain drag. *J. Atmos. Sci.*, **35,** 1644–1654.

Smith, S. M., H. W. Menard and G. Sharman, 1966: Worldwide ocean depths and continental elevations. SIO Ref. G5-8, Scripps Institute of Oceanography, 17 pp.

Starr, V. P., 1948: An essay on the general circulation of the atmosphere. *J. Meteor.*, **5,** 39–48.

——, and R. M. White, 1951: A hemispherical study of the atmospheric angular-momentum balance. *Quart. J. Roy. Meteor. Soc.*, **77,** 215–225.

Swinbank, R., 1984: The global atmospheric angular momentum balance inferred from analysis made during the FGGE and general circulation model experiments. *Quart. J. Roy. Meteor. Soc.*, **109,** in press.

Thomasell, A., and J. Welsh, 1963: Studies of techniques for the analysis and prediction of temperature in the ocean, Part I. The objective analysis of sea-surface temperature. Tech. Dept. Rep. No. 7046-70, The Travelers Research Center, Inc., 52 pp. [NTIS AD 416672].

Trenberth, K. E., and D. A. Paolino, 1980: The Northern Hemisphere sea-level pressure data set: Trends, errors, and discontinuities. *Mon. Wea. Rev.*, **108,** 855–872.

Wahr, J. M., 1983: The effects of the atmosphere and oceans on the earth's wobble and on the seasonal variations in the length of day—2. results. *Geophys. J. Roy. Astron. Soc.*, **74,** 451–487.

White, R. M., 1949: The role of the mountains in the angular momentum balance of the atmosphere. *J. Meteor.*, **6,** 353–355.

Widger, W. K., Jr., 1949: A study of the flow of angular momentum in the atmosphere. *J. Meteor.*, **6,** 291–299.

World Meteorological Organization, 1968: Methods in use for the reduction of atmospheric pressure. WMO Tech. Note No. 91, WMO-No. 226.TP.120, WMO, 21 pp.